Resistance Welding Numerical Simulation

A Promising Technique

Thomas Dupuy* — Chainarong Srikunwong*,**

* Arcelor, Centre de Recherches et de Développements Métallurgiques
rue du Comte Jean, Grande-Synthe, BP 2508, F-59381 Dunkerque cedex 1

{thomas.dupuy, chainarong.srikunwong}@arcelor.com

** Ecole des Mines de Paris
Centre des Matériaux Pierre-Marie Fourt
BP 87, F-91003 Evry cedex

ABSTRACT. *Among welding processes, resistance welding numerical simulation offers the advantage of a direct computation of heat sources through electro-thermal coupling. On the other hand, rare contact input data have to be found or measured. As for other welding processes, the general difficulty in numerical modelling is the availability of input data at all temperatures from room temperature to beyond melting point. Coupling of the first electrothermal models with mechanical models allows a good comparison between simulation and experience. Once a multiphysical validation of a model has been carried out, results like thermal cycles, weld size or residual stresses, strains and metallurgical state can be used for the purposes of process understanding, process control and weld behaviour modelling.*

RÉSUMÉ. *Parmi les procédés de soudage, la simulation numérique du soudage par résistance offre l'avantage d'un calcul direct des sources de chaleur par couplage électrothermique. En revanche, les données nécessaires pour décrire les contacts sont rares et difficiles à mesurer. Comme pour les autres procédés de soudage, la difficulté principale en simulation numérique est la disponibilité de données d'entrée à toutes températures depuis l'ambiante jusqu'au-delà de la fusion. Le couplage des premiers modèles électrothermiques avec des modèles mécaniques permet un bon accord entre expérience et simulation. Une fois qu'un modèle a été validé selon tous les domaines physiques concernés, des résultats comme les cycles thermiques, la taille de soudure ou les contraintes, déformations et état métallurgique résiduels peuvent être utilisés pour mieux comprendre le procédé, pour le commander ou pour modéliser le comportement des soudures.*

KEYWORDS: *resistance welding, numerical simulation, electricity, thermics, contact resistance, coupling, sensibility, validation.*

MOTS-CLÉS : *soudage par résistance, simulation numérique, électricité, thermique, résistance de contact, couplage, sensibilité, validation.*

1. Introduction

1.1. *Welding simulation*

The on-going development of Finite Element Analysis techniques is stimulated by the growing computing power of modern computers. In metal processing, techniques like forming, crash behaviour or casting are now being simulated numerically with a high precision, and commercial Finite Element tools are commonly used in industry to skip experimental tests or to dimension industrial equipments. These applications of numerical simulation techniques allow effective time and cost savings for industrial developments.

In the field of welding simulation, however, the development of such tools was mostly hindered by the fact that welding processes usually imply a number of coupled physical fields:

– For most welding processes (esp. arc and laser), the heating source implies complex phenomena and materials, including high temperature plasmas; numerical simulation of these phenomena is too complex, and therefore the heating source must be evaluated through simplified models, which are usually not universal.

– During welding, materials are subjected to all temperatures from room to beyond fusion, with steep gradients; therefore, welding simulation needs material data at all temperatures, which is either unavailable or very expensive if one wants to be predictive and precise in the results, for an industrial use of the model.

– Eventually, weld properties are mainly defined by the coupled thermal, mechanical and metallurgical processes occurring during the process; if thermal and mechanical phenomena can be rather well modelled, it turns out that the metallurgical simulation is still a growing science, not always able to predict efficiently weld properties.

Though, as explained below these three problems show up specifically when resistance welding simulation is concerned.

1.2. *Resistance welding processes*

The resistance welding processes are characterised by the fact that the heating is provided by the Joule heating effect produced by an electric current flowing through the materials being welded. In the most known resistance spot welding case, current is brought to the weld through a pair of cylindrical electrodes holding together the sheets being welded (Figure 1).
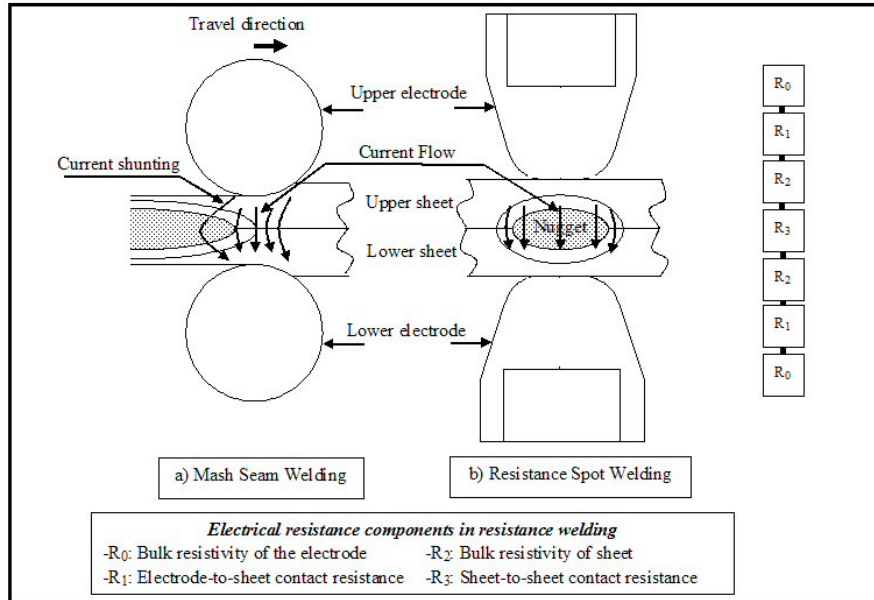
Figure 1. *Resistance welding process principle a) Seam welding, b) Spot welding*

For this process, there are three principal stages as shown in Figure 2:

– Squeezing stage; the sheets are pressed together by the electrodes in order to create the contact. After the force reaches a given value, it is maintained constant in order to stabilise the contact before the welding stage.

– Welding or heating stage; the welding current is applied to the assembly during this phase. The fusion zone and HAZ (Heat Affected Zone) region are generated through Joule heating. The electrical contact resistance at the sheet/sheet interface is responsible for the heating at the beginning of welding. As the temperature in the assembly increases, the contact resistance diminishes rapidly. The development of nugget and HAZ is further governed by the bulk resistivity of sheet.

– Holding or maintaining stage; the maintaining time of the assembly after welding has influence on the cooling rates and the residual metallurgical phases in the weld nugget. The quality and metallurgical-mechanical properties of the weld depend strongly on the duration of this stage.
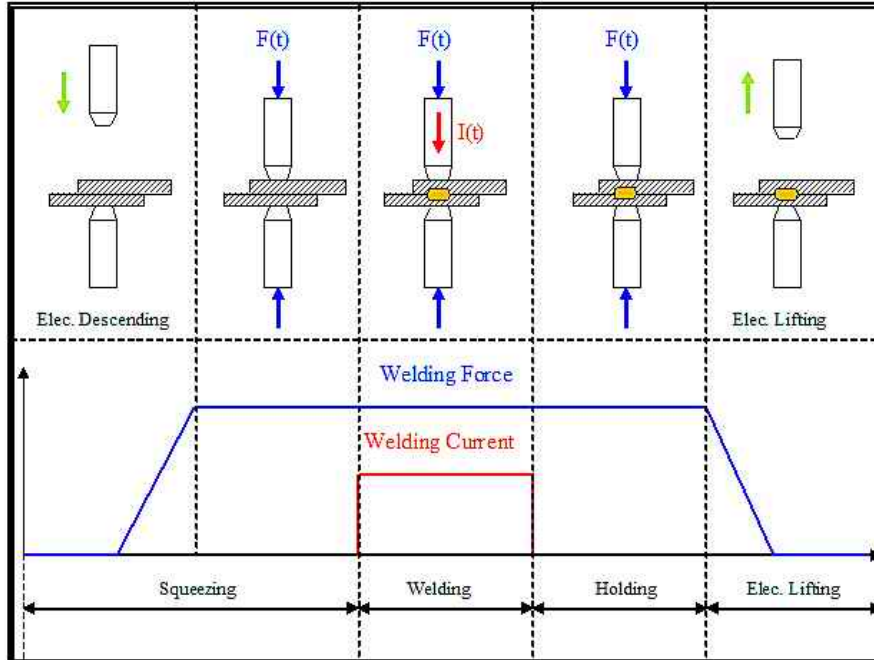
Figure 2. *An illustrated example for the process characteristics of resistance welding, i.e. resistance spot welding process*

Other variants of the resistance welding process include resistance projection welding, for which the electric current concentration is obtained through the local shape of the workpiece, and resistance seam welding, for which a continuous weld can be formed through the rotation of the seam electrodes and the displacement of the welded sheets. Main process parameters in resistance welding are the welding force (the sheets are hold through several kN), the welding current (as high as 10 to 20 kA), and the welding time (usually less than one second) or speed (in the case of seam welding).

1.3. *Resistance welding processes numerical simulation*

In the case of the resistance welding processes, the first problem mentioned above (heating source evaluation) is overcame by the fact that the heating source (Joule effect) can easily be computed through full electro-thermal coupling. In fact, electro-thermal Finite Element models were developed for spot welding for more than 40 years, and more recently coupling with the mechanical aspects of the process was generalized.

However, to be predictive the models must also overcome the second problem (availability of input data at all temperatures), the most problematic input data in resistance welding being the difficult-to-measure thermal and electrical contact resistances, which are of great importance in the first stages of the process (Gedeon *et al*., 1986).

Eventually, obtaining weld properties as a simulation result would be extremely useful in applications like the crash simulation, but this goal implies that the metallurgical history of the weld can be simulated efficiently, so that the model can determine the final weld metallurgical state and mechanical properties. This is the third problem, i.e. availability of efficient metallurgical numerical models.

1.4. *Historical outlook*

Historically, resistance welding simulation first consisted in thermal analysis by using finite difference approach, as found in the literature (Greenwood, 1961, Bentley *et al*., 1963, and Rice *et al*., 1967). Later in 1980's, the first finite element analysis was applied studying resistance spot welding process by Nied (Nied, 1984). Several numerical studies with the use of FE method have been further conducted since then.

Recently, several dedicated softwares, such as SPOTWELDER developed under the general ANSYS$^{®}$ application (Greitman, *et al.*, 1998), SPOTSIM (Sudnik *et al.*, 1999), and SORPAS$^{®}$ (Zhang *et al*., 1998) are commercialised. The objective of these specific resistance welding codes is mainly to provide a global insight of the process variability when the welding parameters are varied. As a result, cost and time reduction can be effectively achieved while designing specific assemblies. In addition, these friendly softwares can easily be used by welding specialists without any numerical experience. However, these codes are only devoted to spot or projection welding.

Other standard commercial finite element codes such as ABAQUS^{TM}, ANSYS$^{®}$ and SYSWELD$^{®}$ are also widely used for the resistance welding processes. In this case, however, a good understanding of the finite element basic formulation and sufficient training are required. The major advantage of the standard code is the variety integration or the coupling for the different complicated analyses between internal phenomena of resistance welding which are the electrical-thermal analysis with the account for the phase transformations due to the thermal history evolution, thermal-mechanical analysis, and the effect of thermo-electric phenomena. Furthermore, the standard code also offers the model flexibility in use for both welding parameters and assembly geometry variety. The meshing topology, the computation criterion and user's developed computation schemes can be selected or implemented by the user.

1.5. *Paper outlook*

Next section of this paper details the difficulties encountered while constructing resistance welding numerical models, as well as the important features for this construction, such as the mesh construction, the thermal-mechanical coupling, and the input data.

Further section deals with the experimental validation of resistance welding models. This stage is essential if one wishes to use the numerical model for predictive purposes (Ferrasse *et al.*, 1998), and it turns out that a more realistic validation must go beyond the simple comparison of the weld nugget size at the end of welding time. It actually involves a feedback loop between the intermediate models and the experimental results (Figure 3). The validation process leads to the optimisation of initial hypotheses and adaptation of input data.

METHOD OF SIMULATION

Process Data + Hypotheses →
- Boundary Conditions
- Material Database
- Mesh Construction
- Heat Source (Mash seam welding case)
→ FE Code SYSWELD® → Model Validation by Comparing with Experience

NOT O.K. → New Hypotheses and Data Corrections

O.K. → Model Validated
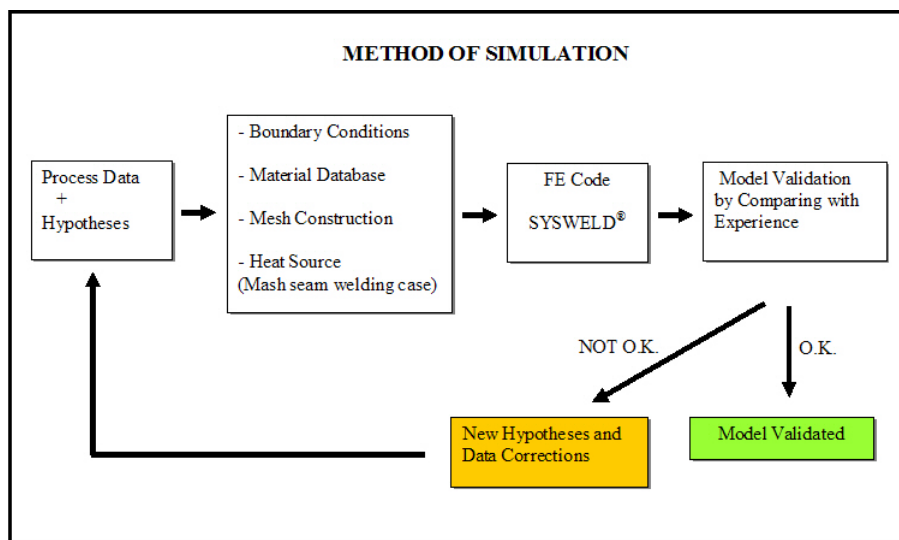
Figure 3. *Method used for mathematical modelling of resistance welding*

Last section is devoted to the model exploitation, since different applications can be developed for such models, including process comprehension, welding parameter or geometry variations exploration, use of the results in other models simulating the weld mechanical performance, and even industrial process control.

2. Model construction

Elaborating a numerical model implies a number of assumptions and decisions concerning the model. These choices relate to four main areas:

– Model geometry and mesh, including the size of the system, the symmetries, and the mesh refinement;

– Coupling degree of the model and equations to be solved, depending on which physical phenomena should be taken into account;

– Boundary condition definition and contact formulation, the latter being fundamental for the resistance welding process simulation, as already highlighted;

– Input data, including physical characteristics and boundary conditions for the system and equations chosen.

Most of this section applies to resistance spot welding, but some important features must be taken into account at this stage for seam and projection welding. These specific points will be highlighted when necessary.

2.1. *Geometry and mesh construction*

The extent of the system included in the model is usually limited to the part of the workpieces to be welded and the welding electrodes. Neglecting the latter would be very limiting, since a number a heat generation and exchanges take place between the electrodes or at the electrode/workpiece interfaces.

On the other hand, extending the system to the whole workpieces or to the welding machine is very costly in terms of computation time, all the more as the symmetries are lost, which implies a three-dimensional meshing instead of the reduced axi-symmetrical two-dimensional mesh that can be used to simulate spot or projection welding. In fact, the simulated system is extended to the machine or the welded structure only in the following cases:

– To study the whole machine behaviour, for instance the electromagnetic fields generated by the power circuit (Silny *et al*., 2001) or the global mechanical deformation of the machine arms (Tang *et al*., 2000 and 2003). However, in these cases the weld itself is not studied precisely.

– To study the workpiece behaviour when subjected to several consecutive welds. Especially, the distortions due to heating and subsequent cooling can be studied as a function of the weld sequence. To limit the computation time, some methods have been developed, allowing to compute each weld individually in 2D with an electro-thermo-mechanical approach, and input the residual stresses and/or distortions into the simplified structure after a 2D->3D transfer procedure (Faure *et al*., 2003).

Mesh construction does not present much difficulty, especially if a 2D structure is chosen. The refinement by increasing the number of elements should be optimised in the nugget and the HAZ regions, where steep temperature gradients are found as shown in Figure 4.
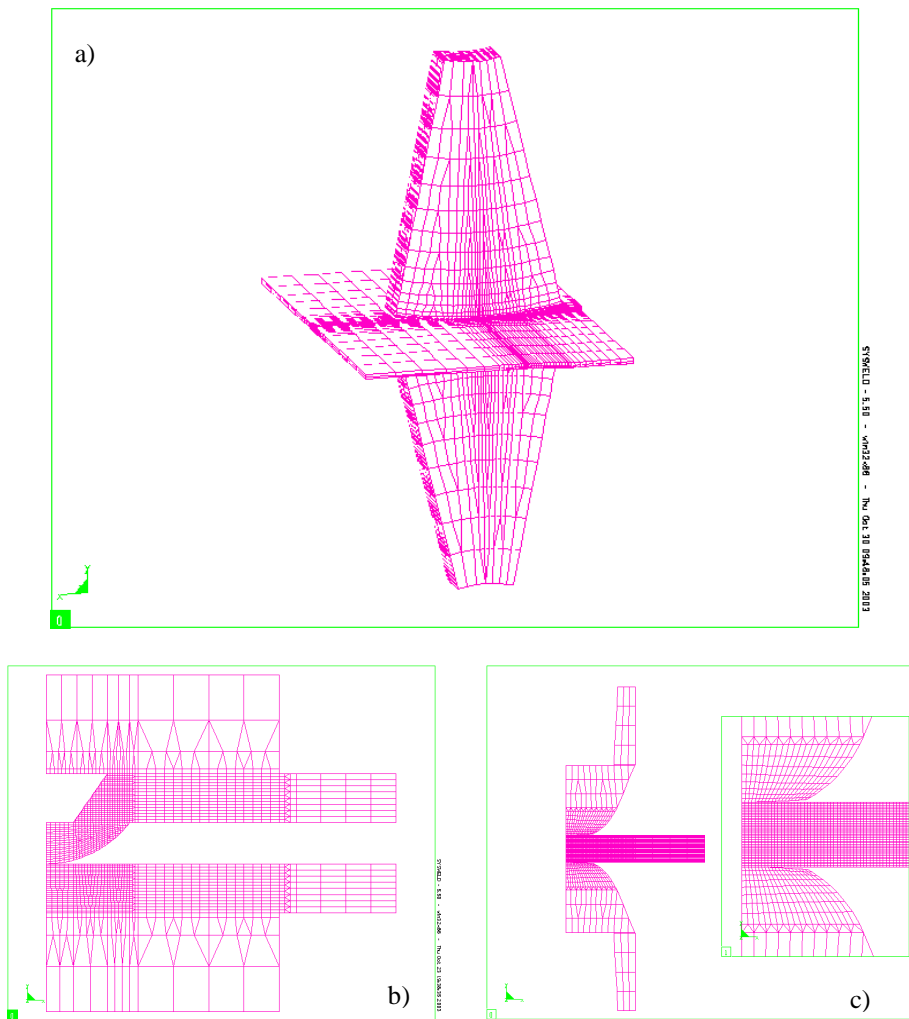
Figure 4. *Mesh examples a) Mash seam welding 3-D mesh construction b) Projection welding 2-D mesh construction c) Resistance spot welding 2-D mesh construction. Refinement for the number of elements in the weld and the HAZ regions where steep thermal, stress and deformation gradients occur*

For resistance welding, special contact elements must be introduced to account for the thermal and electrical contact resistances (see dedicated section below). These elements are placed at the electrode-to-sheet and sheet-to-sheet interfaces. The contact resistance can be represented in two ways:

– Creating a thin artificial contact layer between the contacting surfaces. The thickness of these supplementary elements is in an order of micrometers. To account for the electrical contact resistance, the resistivity of the layer is defined in $\Omega.m$ (Huh *et al.*, 1997, Thièblemont, 1992).

– Some commercial finite element codes, such as ABAQUS™ or SYSWELD[®] offer special electrical-thermal contact elements, described later. The magnitude of the electrical contact resistance is then defined directly in $\Omega.m^2$.

In our projection and resistance spot welding models, special electrical-thermal contact elements of SYSWELD[®] are introduced at the interfaces.

The case of seam welding simulation, however, is completely different from the spot and projection welding standard configuration, mainly because there is a displacement between the seam electrodes and the welded sheets. This dynamical aspect is not impossible, but complex and time-consuming to model. Another alternative to take this dynamical aspect into account is to consider the process as quasi-static, which is possible in the case of continuous cycle welding only. In addition, the weld is not axisymmetrical. Even if symmetry planes or lines allow a reduction of the model size (which is the case only in some configurations), and if the seam may be reduced to an angular segment, a heavy 3D-structure mesh as shown in Figure 4a must be constructed to simulate the process. The problem is even more complex in the case of mash seam welding, since the sheets are much deformed during welding: modelling this process correctly needs mechanical-thermal coupling (see further).

Some 2D simplified models have been elaborated to simulate seam welding (Ferrasse *et al.*, 1998). Although a 2D cut in the seam electrodes plane could be interesting to study the electrical current repartition between the upstream and downstream parts of the weld, the cutting plane is usually the transverse plane. In this case the weld section studied must have a pre-defined geometry, either constant (which is an important simplification in the case of mash welding) or with a pre-defined deformation deduced from experimental observations. It is thought that a coupled model combining both 2D cuts could be efficient: a longitudinal model (cut in the seam electrodes plane) can be used to compute the current repartition between up- and downstream parts of the weld (assuming that temperatures and voltages are constant through the thickness of the seam electrodes); then a transverse model using this current repartition as input could compute the thermal build up in a sheet section travelling across the seam electrodes region.

2.2. *Physics coupling and governing equations*

The general physics of the resistance welding modelling schematised in Figure 5 reveals the relevant aspects such as the heat transfer, mechanics, metallurgy, and electro-magnetokinetics.
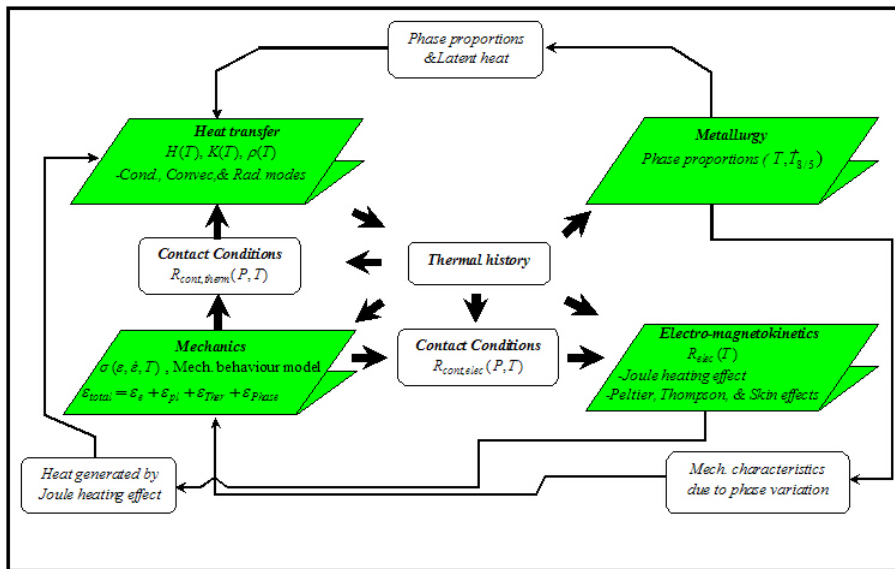
Figure 5. *Interactions among different physical phenomena in resistance welding*

2.2.1. *Electro-thermal equations*

Like for any other welding process, heat transfer can be described by the heat conduction in the assembly, air-convection and radiation at the outer surfaces and the cooling water inside the electrode. Though, it as said above that for resistance welding the heating source, *i.e.* Joule effect, can be computed directly through full electro-thermal coupling. It is found in the literature (Thièblemont, 1992) that electrodynamic phenomena can be neglected, leading to the following governing equations for the electro-thermal phenomena:

$$\rho \frac{\partial H}{\partial t} - div(\lambda.\mathbf{grad}T) - \mathbf{grad}V.\sigma.\mathbf{grad}V - Q = 0 \qquad [1]$$

$$div(\sigma.\mathbf{grad}V) = 0 \qquad [2]$$

where $T, \mathbf{V}$ are the temperature and the scalar electrical potential, respectively. ρ, λ and σ represent the density, the thermal conductivity and the electrical conductivity of the considered media and the temperature dependency characteristic can be taken into account. H is the enthalpy with temperature dependency. The fully coupling between electrical and thermal phenomena can be governed by the term $\mathbf{grad V}.\sigma.\mathbf{grad V}$ in the heating equation which is represented the Joule heating effect.

In the special case of simplified 2D seam welding modelling, the model may be only thermal without the electrical coupling. However, in this case the heat sources have to be correctly evaluated and located in the weld region, which is not an easy task (Ferrasse *et al.*, 1998).

Metallurgical phenomena can be introduced and fully coupled with electrothermal phenomena through additional variables describing the metallurgical state of material welded, i.e. grain size, precipitation parameter, percentage of phases, etc… depending of which phenomena are important physically. Electrothermal properties have to be defined as functions of these variables (for instance the electrical conductivity has to be given for each metallurgical phase or as a function of grain size), and constitutive laws ruling these additional variables must be introduced. As far as welding is concerned, these laws are mainly a kinetic description of the metallurgical phenomena like phase changes, precipitation, grain growth, etc… as a function of the thermal cycle. SYSWELD is one of the main softwares allowing the user to introduce metallurgy in welding simulation as phenomena fully coupled with electrothermal equations.

2.2.2. *Mechanical coupling*

The mechanical aspects can be taken into account through a classical elastoplastic formulation, but the behaviour of high temperature material may be better represented through a viscoplastic behaviour. Beyond melting point the material behaviour should be represented with a liquid formulation, but in commercial codes it is usually not possible to change behaviour laws when temperature changes. A formulation must then be chosen for all temperatures, and the different behaviours have to be represented through variation of parameters with temperature. If metallurgy is taken into account, of course, the behaviour must be defined as a function of the metallurgical state of the material. This can be a possibility to better describe the specific liquid behaviour, as a new metallurgical state.

The coupling degree between mechanical and electrothermal analysis can vary from none to fully coupling:

Fully decoupled procedure can be described by transferring the nodal thermal history from the electrical-thermal analysis to the thermal-mechanical calculation once the electrical-thermal analysis terminates. The mechanical analysis is then carried out by using the whole thermal history, leading to residual strain and stress evaluation.

The advantages of this fully decoupled procedure are the low computational cost and the simplicity of the computation scheme between two modules. However, this decoupled procedure does not take into account the significant variation of the contact size at electrode-to-sheet interface and faying interface. The contact variations during welding have a strong impact on heat generation by Joule effect at the contacts, especially when curved-face electrodes are used. In addition, the significant collapse of the assembly is not reproduced in the projection welding simulation case.
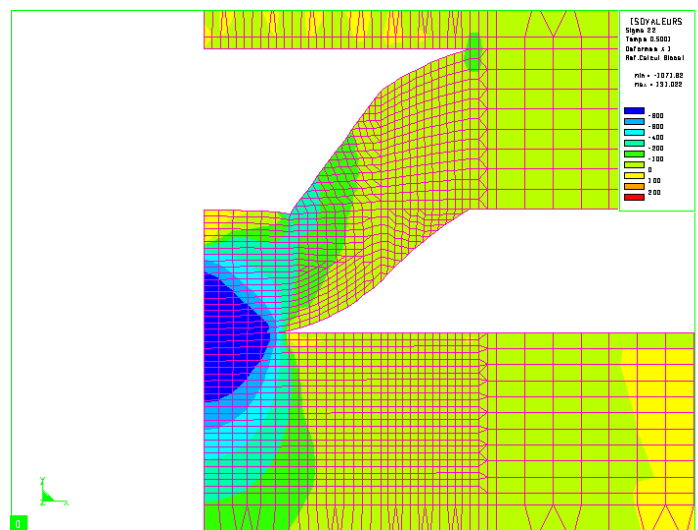
Figure 6. *Contact stress at the end of squeezing stage in the case of projection welding welding simulation*

To make the simulation possible for projection welding and joining sheet with various electrode face profile in case of spot welding, a coupled procedure was developed. The basic concept of this computation scheme is to update the deformation of the assembly by using a sequential computation loop between the two modules. As in the fully decoupled procedure, the thermal history from the electrical-thermal analysis is transferred to thermal-mechanical analysis in order to take into account the temperature dependency characteristic of material. On the other hand, the deformation of the assembly and contact pressure resulting from thermal-mechanical computation are transferred back to the electrical-thermal analysis at several stages of the process. This coupling procedure is illustrated in Figure 7.
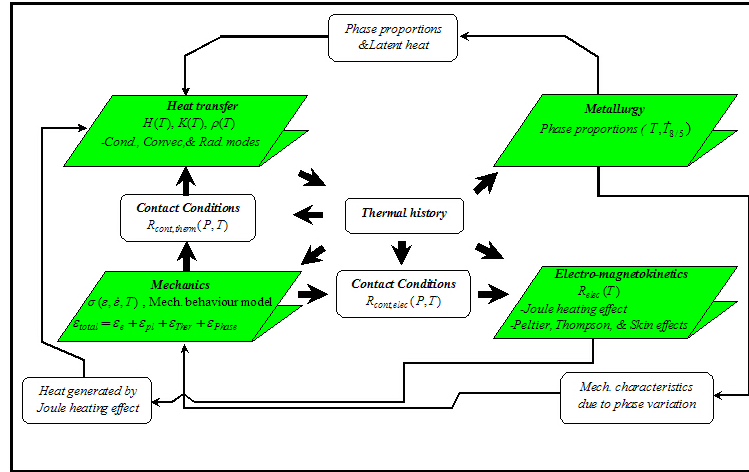
Figure 7. *Illustration of the coupling procedure used in the spot welding simulation*

However, different coupling levels can be high-lighted, regarding to time-step for assembly geometry updating:

– Geometry updating each macro time-step (Figure 7a); the macro-time steps (for example 50 Hz periods) are defined equivalently in both electrical-thermal and thermal-mechanical analyses. However, the micro time-step scale for both modules may be different.

– Geometry updating for each micro time-step as depicted in Figure 7b; the time-step have to be equal in both macro and micro scale for both electrical-thermal and thermal-mechanical analyses.

– Fully coupling for each micro time-step between two analyses as shown in Figure 7c; In this case convergence must be reached simultaneously for both analysis at each micro-time step.

2.3. *Boundary conditions and contact formulation*

2.3.1. *Boundary conditions*

The electrical-thermal and thermal-mechanical boundary conditions for resistance welding are shown on Figure 8 and Figure 9, and explained below:

– $\partial\Omega_1$ and $\partial\Omega_9$: Water-cooling sink surfaces for the electrical-thermal analysis;

– $\partial\Omega_2$: Section area of the upper electrode subjected to the welding current flux for the electrical-thermal analysis and imposed pressure for the thermal-mechanical analysis;

– $\partial\Omega_3$, $\partial\Omega_5$, and $\partial\Omega_7$: Free surfaces for air convection in the electrical-thermal analysis;

– $\partial\Omega_4$ and $\partial\Omega_6$: Free surfaces where the combination of radiation and air convection heat transfers by using an equivalent heat transfer coefficient;

– $\partial\Omega_8$: Section area of the lower electrode subjected to the zero potential for the thermal-mechanical analysis and the constrained nodal displacement in axial direction for the thermal-mechanical analysis (in y-direction).
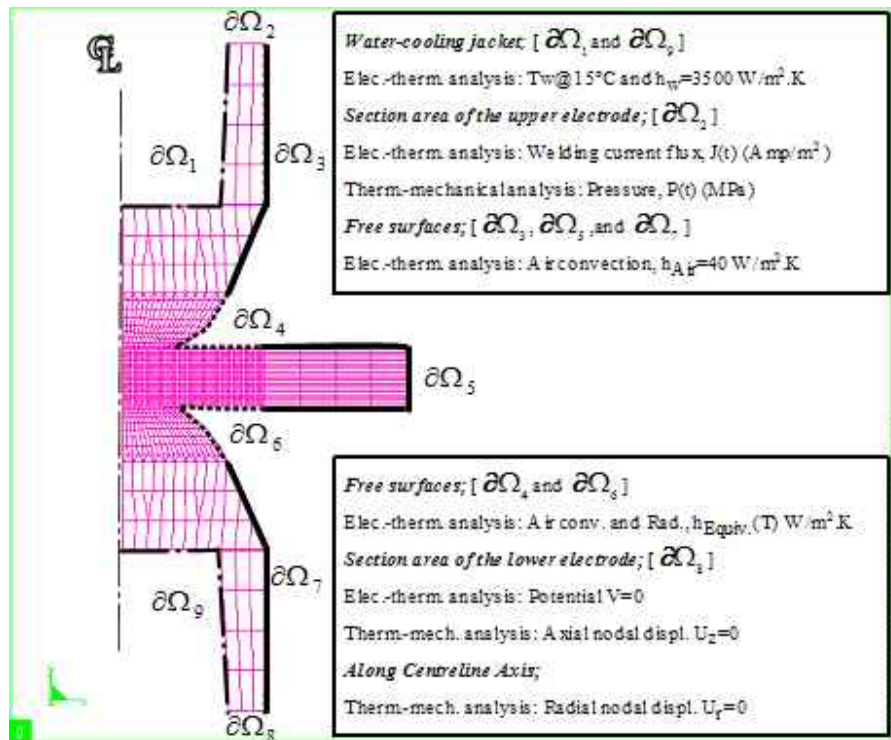
Figure 8. *Demonstration of the boundary conditions for the electrical-thermal and thermal-mechanical computations used in the resistance spot welding*

Before the beginning of welding cycle, the electrical initial conditions are set equal to zero, while the temperature of entire structure is specified as the room

temperature. During the welding cycle, the welding current is applied at the top of the upper electrode and zero potential is specified at the bottom surface of the lower electrode. Consequently, the current flows from the upper electrode, passes through workpiece and terminates at the bottom annular section of the lower electrode.

The electrode force is modelled from the experimental welding force signal by assuming a uniform pressure distribution across the annular end of the upper electrode. The vertical nodal displacement of the annular end of the lower electrode is constrained corresponding to the welding operation with the pedestal welding machine. Some more sophisticated mechanical boundary conditions can be used to include the machine mechanical response into the model, since this parameter may have a great influence on weld formation, especially in the case of projection welding (Vichniakov *et al.*, 2001).
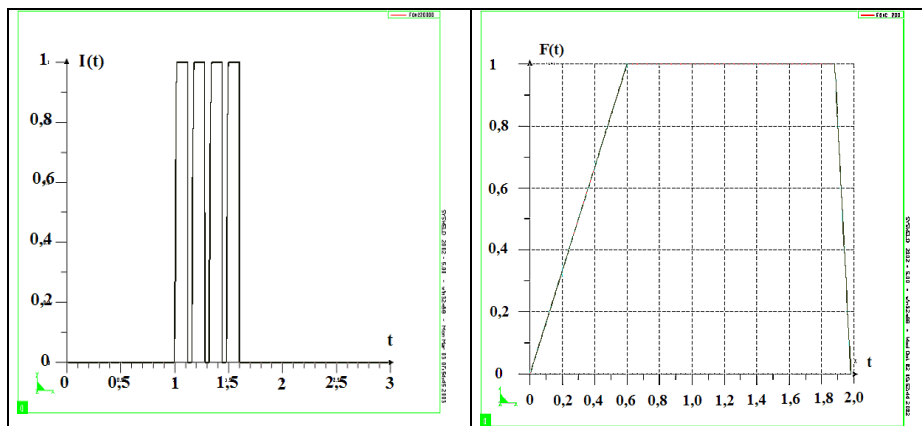
Figure 9. *a) 4-pulse welding current schedule used in simulation. b) Welding force as a function of time showing squeezing, welding and holding stage*

2.3.2. *Contact formulation*

In addition to classical boundary conditions, the contact formulation (mainly electrical-thermal) is very important in resistance welding simulation.

2.3.2.1. Electrothermal contact

During the low temperature stage of the process, main part of the Joule heat is generated through contact electrical resistances at electrode/sheet and sheet/sheet interfaces, because the contact electrical resistance is higher than the bulk resistivity at lower temperatures. The heat generated at the interface is then propagated in the weld structure. As the temperature increases, the electrical contact resistances are dramatically diminished, but the bulk electrical resistivity of sheet is increased, and thus governs the heat generation in the assembly for the latter stages of welding.

As said before, this "interfacial resistivity" can be taken into account through a very fine layer of massive elements, whose high electrical resistivity (at low temperature) is chosen to represent the electrical contact resistance. However, a contact thermal resistance is also active at these interfaces, so that a high thermal resistivity must also be chosen in these layers. In this case, an artefact is that all the Joule heat generated in these elements at low temperature cannot be conducted into the structure because of very low thermal conductivity in these contact elements, and builds up locally, which is not physically reasonable.

Therefore, electro-thermal contact formulation with special contact elements is preferred. Actually, actual electro-thermal interaction at an interface is a physically complex problem, still under discussion (Le Meur, 2002). For instance, the contact resistance dependency with temperature must be irreversible, since the better electrothermal contact obtained through heating will remain in case of cooling back the interface, because this dependency is linked to the plastic squeezing of local contact asperities. Therefore, even if not fully exact with respect to theory, electro-thermal contact formulation must be precise. A good description of such a formulation is given elsewhere (Robin *et al.*, 2001). In this formulation, the Joule power dissipated at the interface because of contact resistance is usually partitioned between the surfaces according to the empirical rule of effusivity ratio, which is a good approximation even if the actual partitioning may be different (Le Meur, 2002).

2.3.2.2. Mechanical contact

For the mechanical contact formulation, a node-to-node contact may be sufficient in first approach since the tangential relative displacements between the surfaces are limited, at least for spot welding. However for projection welding a generalised surface-to-surface contact formulation is almost mandatory.

At low temperature the contact is to be considered gliding, with friction if data are available, but this parameter does not influence much the results. This is not the case when temperature reaches the melting point of the material. Physically, the mechanical contact doesn't exist anymore, but the fluidity of the liquid metal is best represented through a gliding contact. After solidification, *i.e.* actual welding of the surfaces, the contact should become sticking to be representative. In commercial codes, however, mechanical contact properties are usually not dependent on thermal history.

2.4. *Input data*

2.4.1. *Electrical-thermal input data and sensibility study*

2.4.1.1. Material data

Using the enthalpy model for the electrical-thermal analysis, the enthalpy of steel sheet can be determined from the integration of specific heat of the

ThermoCalc® measurement, taking phase changes latent heats into account. Enthalpy beyond the fusion temperature of steel is linearly extrapolated. Similarly for the bulk electrical resistivity evaluation, a linear extrapolation is used for elevated temperatures.

For welding simulation, there are two methods to evaluate the thermal conductivity beyond fusion temperature:

– a linear extrapolation technique and the use of the value of pure iron at elevated temperature in case of the ferritic low-alloy carbon steel property estimation (Bobadilla *et al.*, 1994);

– an increase of thermal conductivity after $T_{solidus}$ in order to compensate the convection effect in weld pool (Watt *et al.*, 1988, Vogler, 1992).

2.4.1.2. Contact data

For the resistance welding process simulation, the other significant input is the contact characteristic of both electrode-to-sheet and sheet-to-sheet interfaces. The global dynamic electrical resistance of the assembly can be commonly monitored as a function of time. However, it is not an easy task to decompose this global dynamic resistance of the assembly into individual resistance component including contact resistances and correlate the contact resistances with the corresponding interface temperature (Thièblemont, 1992).

The measurement of the electrical contact resistance at different conditions of contact pressure and temperature was conducted and reported by (Vogler, 1992). It was found that the contact resistance depends strongly on the contact surface hardness, temperature, and loading pressure. Recently, an empirical mathematical model described as a pressure/temperature dependent function is proposed in the literature (Babu *et al.*, 2001).

In this study, measured electrical contact resistances from Thièblemont, 1992 are introduced to the electrical-thermal model. To take into account the hysteresis characteristics of the contact resistance due to contact temperature evolution, this temperature dependency electrical contact function depends on the highest temperature reached at the interface during the process (Dupuy *et al.*, 2000 and Vogler *et al.*, 1993). According to literature, it is believed that the contact resistance drops abruptly with the temperature and shows an insignificant change at elevated temperature as shown in Figure 10d.
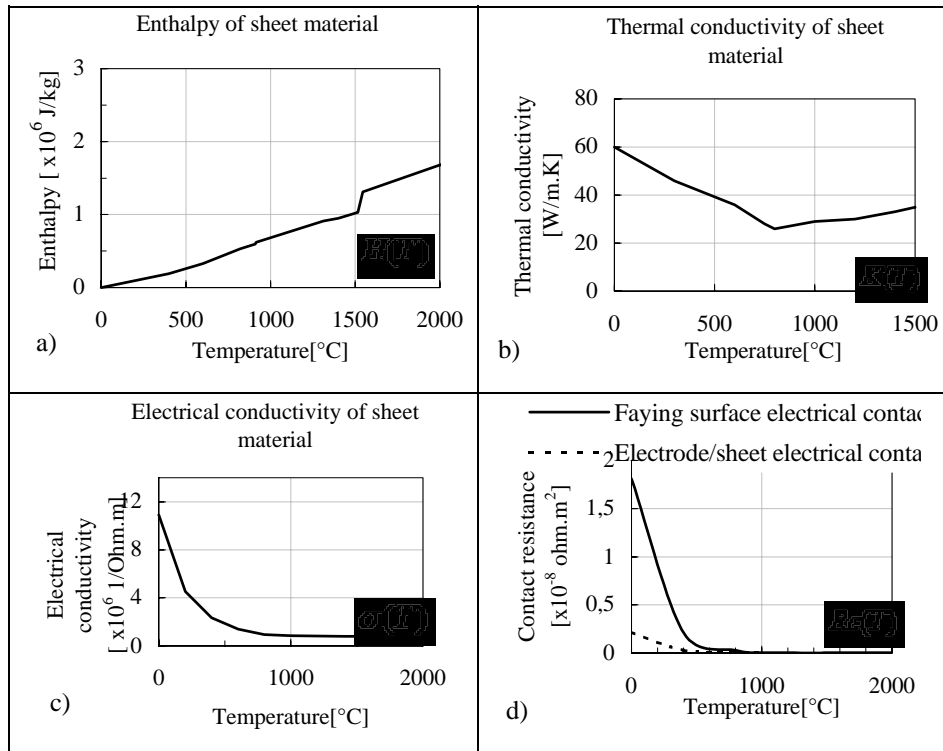
Figure 10. *Electrical-thermal property data as a function of temperature introduced to the model for non coated low-carbon Al-killed drawing quality steel sheet, a) Enthalpy, b) Thermal conductivity, c) Electrical conductivity, and d) Electrical contact resistance at the interfaces*

2.4.1.3. Sensibility study

The influence of electrical-thermal input data variability was studied numerically through variations of +/-5% of the properties magnitude in a two-sheet configuration case. In this study the degree of variation for electrical contact resistance was brought up to +/-20% because it is widely agreed that it has a strong impact on the nugget and HAZ development. The influence of the electrical/thermal material property is discussed on the nugget and HAZ size and geometry.

The summarised details of thermal/electrical property variation influencing weld geometry is shown in Figure 11. It is disclosed that the sheet electrical conductivity is the most significant input influencing on the weld geometry among other thermal parameters. The decrease in thermal conductivity, enthalpy or electrical conductivity results in the enlargement of the weld geometry. Increasing electrical contact resistance also results in larger final nugget and HAZ geometry, but less significant influence comparing to those of other thermal parameters.
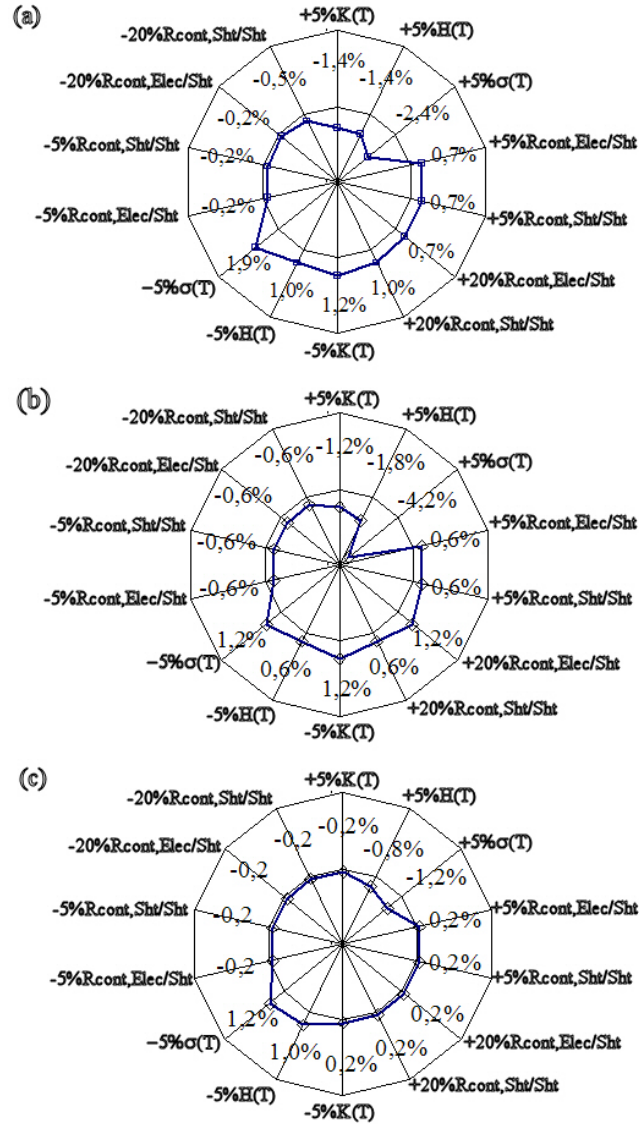
Figure 11. *Comparison of the relative variations in nugget and HAZ geometry at the end of welding due to* $\pm 5\%$ *variation of thermal-electrical properties and* $\pm 20\%$ *variation for the contact characteristics; (a) relative final nugget diameter size (b) relative final penetration height and (c) relative final HAZ diameter measured at the faying surface. Welding conditions 2 mm DQ steel, TH8 electrodes, welding force 400 daN, welding time 4(6+2), direct current 11,2 kA*

Actually, the electrical contact resistance plays a great role on the weld geometry development at the early welding stage, as demonstrated in Figure 12. Additionally, the sensibility of the predicted nugget and HAZ diameter sizes due to the electrical/thermal property variability shows a similar tendency as shown in Figure 11c.
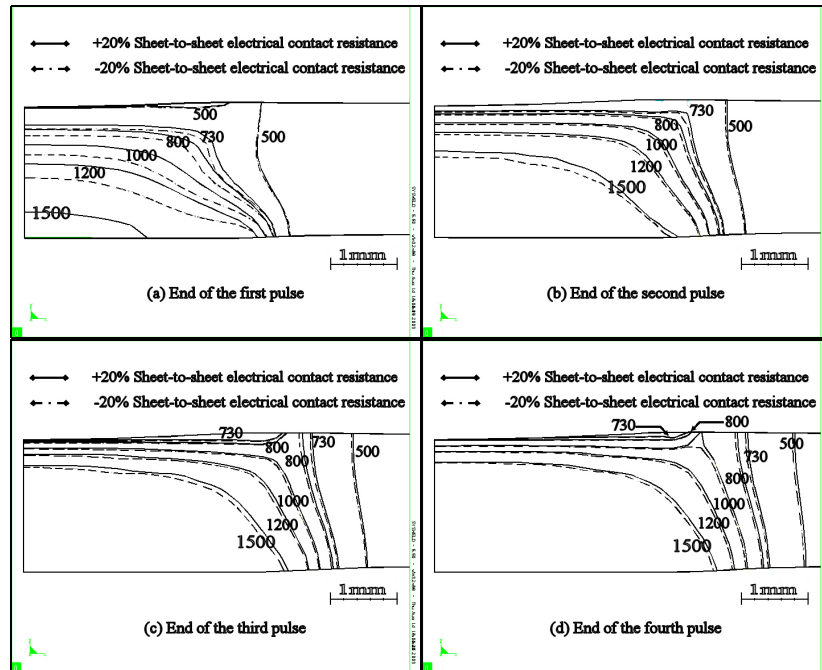
Figure 12. *Nugget and HAZ geometry due to ±20% variation for the electrical contact resistance; (a) after one pulse (b) after two pulses (c) after three pulses (d) at the end of welding. Welding conditions 2 mm DQ steel, TH8 electrodes, welding force 400 daN, welding time 4(6+2), direct current 11,2 kA*

2.4.2. *Metallurgical data*

As it was written above, in the metallurgical field one needs data on metallurgical transformation kinetics. Such data do exist in a normalised form, for instance CCT diagrams for steels. However, difficulties arise for resistance welding simulation, because in these processes heating and cooling rates are much higher than those used in established diagrams, and even too high to be reached with the most powerful experimental devices for this kind of experiments. Resistance welding heating and cooling rates can only be approached, which may be sufficient since a number of metallurgical reaction rates tend to a limit at high heating or cooling rates.

2.4.3. *Thermal-mechanical input data*

If the constitutive laws for materials are easy to measure or find in literature for room temperature, the task becomes much more difficult when the temperature rises, since the tests are more complex to carry out, and the high temperature viscoplastic behaviour needs more tests to be identified.

3. Model validation

Experimental validation of a numerical model is a fundamental stage if one wants to use this model in a predictive way. Usually, spot welding numerical models are mainly checked through comparison of the final weld size comparison between model and experiment (Figure 13). Numerically, attention must be paid to the fact that the molten zone limit may not be exactly the fusion temperature isotherm at the end of welding time, since locally some material may melt through heat diffusion only after current shut off, especially if complex cycles are used (see example with HAZ size in next section). Experimentally, the molten zone diameter may be evaluated from nugget plug nominal diameter size, but a macro-photography of the sectioned weld give better results. Both techniques are combined by Vogler, 1992.
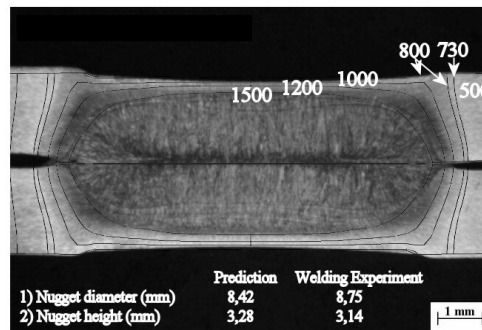
Figure 13. *Validation of nugget final size for two-sheet joining (@2mm-thick ES grade, welding schedule 400daN-11.2kA/4(6+2)-TH8)*

However, it turns out that the weld size criterion is not very discriminating, since there is a wide range of conditions for which the weld diameter is around the electrode diameter, and the weld height is around 80-90% of the cumulated sheet thickness. Of course, a representative final weld size is the first point to check for a

model, but this result is not enough, especially if one wants to use the model as explained in next section.

Among the other parameters that can be observed, quantified and compared between experiment and model, one can notice:

– the Heat Affected Zone (HAZ) size, also shown on Figure 13;

– the heated zone development during welding time (kinetic aspect);

– voltage between electrodes (if current is fixed);

– relative axial displacement of electrodes during welding, which can be measured experimentally through an adapted sensor; electrode displacement may be specially useful in the projection welding case;

– final deformed shape of the weld zone, including electrode indentation into the sheets and projection final collapse in the projection welding case;

– residual stresses, whose experimental measurement is not an easy task in the small confined area around a spot weld.

An example of nugget development kinetics validation through macrographs after interrupted welding cycles can be found in the literature (Srikunwong *et al.*, 2003). For the same kinetic aspect, an example is presented thereafter with temperature cycle comparison during welding.

For recording thermal cycles in the weld zone, infra-red thermography during welding process can be conducted by using a camera in the case of mash seam welding, because the hot surface just after welding is left visible thanks to seam displacement (Ferrasse *et al.*, 1998).

For the resistance spot welding and projection welding, thermal cycles can be recorded through micro-thermocouples embedded in the electrodes or even in the sheets. The validation of thermal history by the implantation of micro-thermocouples in the lower electrode was carried out for ten welding spots and the measured thermal cycles were then averaged for each local position. Several numbers of welding operation and thermal cycle measurements help assuring the reproductive and comparative results. The experimental procedures can be found elsewhere (Le Meur, 2002). The welding condition according to the French welding standard (ISO, 2003) and the sheet material used are given in Figure 14. A single pulse schedule of ten welding cycles is applied for this joining case. The predicted thermal history shows a good qualitative agreement with the experience for both heating and cooling stages of the process. Slightly higher heating and cooling rates at the early and final stages of welding can be observed in the numerical results. This example shows that even if the thermal state at the end of welding is satisfactory (same nugget size, same maximal temperature in electrode), the kinetic of the process may be wrong, which is of first importance for metallurgical reaction evaluation, for instance.
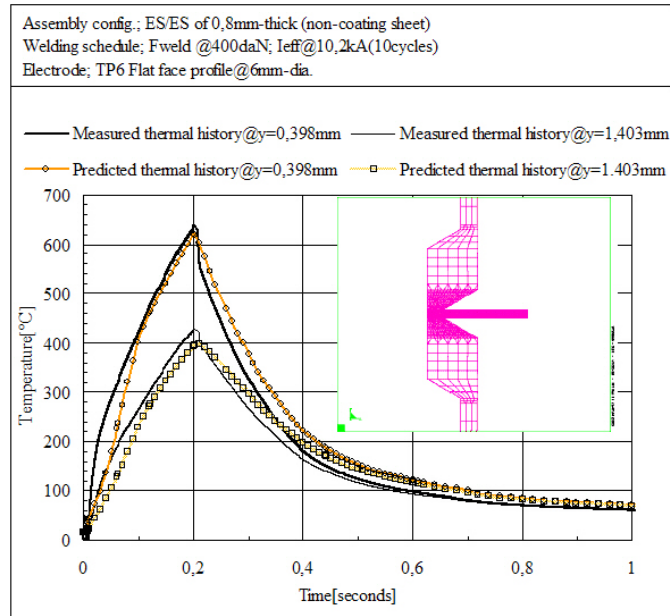
Figure 14. *Validation of thermal history at different positions in the lower electrode*

Welding conditions		Welding current	Welding force	Study features
Elec. dia. (mm)	Assembly configuration	[kA-Type/N° of pulse]	[daN]	
1) TH6		8.97-DC/4(6+2)	400	*
2) TH8		10.6-DC/4(6+2)	450	**
3) TH8		11.2kA-DC/4(6+2)	400	***
4) TH6		7.80-AC/3(7+2) +6.5kA×17 (post-heating pulses)	500	*
5) TH6		8.62-DC/1(8)	230	**
6) TH6		8,63-DC/1(8)	270	**
7) TH8		9,08-DC/1(8)	230	**
8) TH6		7,36-DC/1(8)	230	**
9) TH6		7,55-DC/1(8)	230	**

Sheet grade used: - ▧▧▧▧▧ *2-mm thick ES sheet*
                         - ▭▭▭▭ *0,8-mm thick IF-Ti sheet*
                         - ▨▨▨▨ *1,46-mm thick TRIP800 sheet*
Simulation and study the process influence on thermal aspects of a spot weld
** Kinetic macro-photograph validation*
*** Sensibility study and kinetic macro-photograph validation*

Table 1. *Welding configurations tested for the model/experiment comparison*

More generally, model validation (comparison with experience) should always be multiphysical and cover a given range of welding configurations and conditions, defining the welding conditions area for which the model is worth of confidence. In our case, the configurations tested are summarized in Table 1. The multiphysical model-to-experiment comparison results allow a good evaluation of the model weaknesses and orient the corrections that can be brought to input data or physical formulation to make the model better. For example, in our case the thermal results show that the global heating is lower in the model than in experiments, especially at the beginning of the process. This general result found for all configurations made us examine the contact formulation and data and program some new contact resistance measurements.

4. Model exploitation

The most common and immediate use for a numerical model of spot welding is to extract thermal cycles seen in the welded sheets or in the electrodes, since the experimental measurement of such temperatures is a difficult task. Such thermal cycles may be required to solve different problems:

– Temperatures reached in the electrodes have a great influence on their degradation, and can be used to evaluate diffusion coefficients or to determine which phase form onto their surface (Dupuy, 1998).

– With a numerical model the magnitude of the thermoelectrical Peltier effect in spot welding was evaluated compared to Joule effect (Dupuy *et al.*, 2000).

– The model developed by Arcelor was also applied to the case of weldbonding: through extracting the thermal cycle between the sheets, it was possible to evaluate until which distance from the weld the adhesive material could have been cured or decomposed by the welding cycle.

– Another example of thermal cycle exploitation is detailed now. The nugget geometries and sizes at the end of each pulse in the case of TRIP steel joining are illustrated in Figure 15. It is obvious that the nugget develops until the end of pulsed welding. The peak temperature at the weld centre and at any other node on the axis is found at the end of the last (third) pulse (Figure 16c). A temperature drop can be observed during the current shut-off. The temperature at the axial nodes increases again during the post-heating stage but with a lower heating rate than experienced during welding. In the same way, the molten zone is not enlarged during post-heating stage, its maximum size has been reached at the end of third pulse. This is in contrast to HAZ size and radial temperature evolution during this additional post-heating stage. Actually, it can be seen that the HAZ diameter is significantly increased during post-heating stage (Figure 15d), and that this region along the axial direction continues to heat up, reaching its maximal temperature even after the post-heating stage is finished. In this case, the model is useful to understand in detail the effects of a post-heating cycle.

– In the latter case, thermal cycles in the sheet were actually used to simulate the metallurgy state reached in different HAZ regions of the weld with a Gleeble Machine.
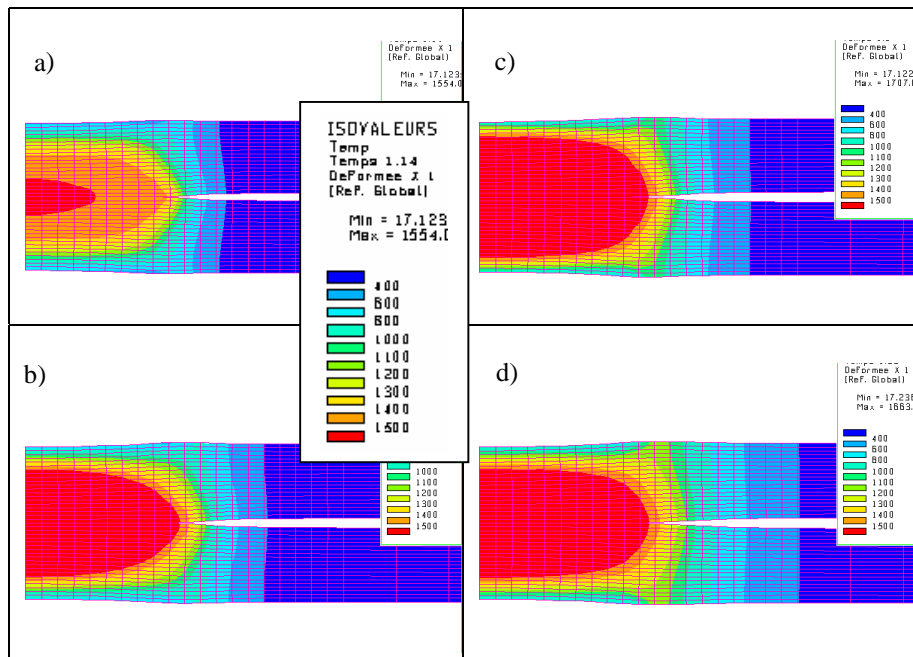
Figure 15. *Predicted nugget and HAZ development kinetics using post-heating current with welding schedule 7.8kA-AC/3(7+2)+6.5kA×17 - 500 daN for joining TRIP800 steel sheets a) End of the first pulse, b) End of the second pulse, c) End of the third pulse and d) End of post-heating (Srikunwong* et al., 2003).*

Another application for a numerical model of spot welding is linked to on-line monitoring and control of the process (Matsuyama *et al.*, 2002). For this purpose, calculation must be very fast. The method includes a Finite Difference model using on-line measured voltage and current input to evaluate a global electrical resistance of the assembly. The output of the model is a weld size, and depending of the calculation time the welding schedule may be adapted for the next weld or even for the on-going weld, though welding time shortening or lengthening. Another example of such a control device using a numerical model is given by Tsai *et al.*, 1991.

Last but not least, the main application of spot welding numerical model results in the coming years may be their input in numerical models made to study the stiffness or crash behaviour of global structures (Hahn *et al.*, 1999). This kind of

application has already been approached above with the example of global distortion study. The 2D local results of a spot welding model (i.e. residual deformations, residual stresses and/or resulting metallurgical state) have to be transferred to 3D or shell elements. This transfer usually includes a simplification to reduce the number of elements and nodes representing the weld. However this full procedure, which allows a coupling between welding parameters and the weld behaviour inside the global structure, is not yet much applied. Though, this kind of transfer procedure was already applied to model the behaviour of normalised testing coupons (Koppenhoefer *et al.*, 2000).
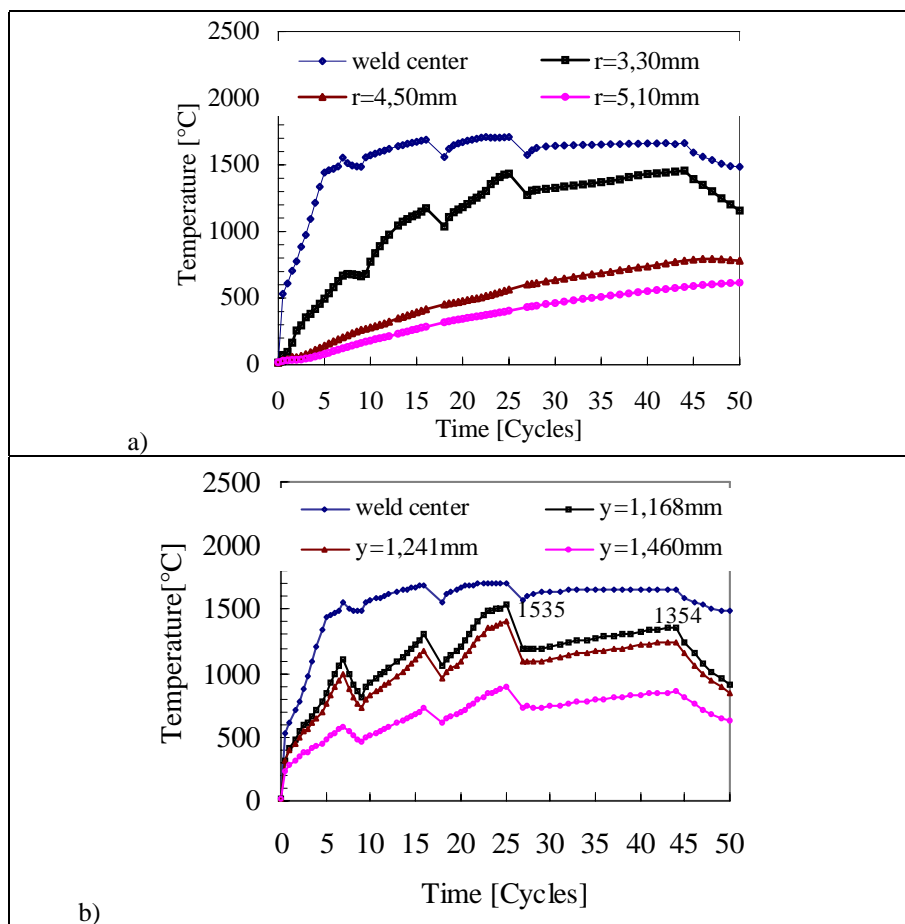
Figure 16. *Influence of post-heating current on temperatures at the end of welding with welding schedule 7.8kA-AC/3(7+2)+6.5kA×17 - 500 daN for joining TRIP800 steel sheets a) Average thermal history at different radial positions, b) Average thermal history at different axial positions.*

5. Conclusion

Among welding processes, resistance welding numerical simulation offers the advantage of a direct computation of heat sources through electro-thermal coupling. On the other hand, rare contact input data have to be found or measured. As for other processes, the general difficulty in numerical modelling is the availability of input data at all temperatures from room temperature to beyond melting point. Coupling of the first electro-thermal models with mechanical models allows a good comparison between simulation and experience. Once a multiphysical validation of a model has been carried out, results like thermal cycles, weld size or residual stresses, strains and metallurgical state can be used for the purposes of process understanding, process control and weld behaviour modelling.

6. References

Babu S.S., Santella M.L., Feng Z., Riemer B.W., Cohon J.W., "Empirical model of effects of pressure and temperature on electrical contact resistance of metals", *Science and Technology of Welding and Joining,* 2001, vol. 6, p. 126-132.

Bentley K.P., Greenwood J.A., Knowlson P. McK., Baker R.G., "Temperature distributions in spot welding", *British Welding Journal*, Dec. 1963, p. 613-619.

Bobadilla M., Niederleander M., Nuss C., Perrin G., Selaries J., « Données thermiques pour différentes familles d'acier », *Internal Report of IRSID*, Group Arcelor, June 1994.

Dupuy T., "The degradation of electrodes by spot welding zinc coated steels", *Welding in the World*, vol. 43, n°6, p. 58-68, 1998.

Dupuy T., Ferrasse S., "Influence of the type of current and materials properties on resistance spot welding: Using a finite element model", *Trends in Welding Research 5*, Pine mountain, GA., 1998.

Dupuy T., Fardoux D., "Spot welding zinc-coated steels with medium-frequency direct current", *Proceeding Sheet Metal Welding Conference IX*, AWS, M. Kimchi and W. Newman, eds., oct. 2000.

Faure F., Souloumiac B., Bergheau J.M., Leblond J.B., "Prediction of distortions of large thin structures during welding using shell elements and multiscale approaches", *7th International Seminar Numerical Analysis of Weldability*, Graz-Seggau, Austria, 29th sept.-1st oct., 2003.

Ferrasse S., Piccavet E., "Thermal modelling of the mash seam welding process using FEM analysis", *Mathematic Modelling of Weld Phenomena IV*, H. Cerjak and H.K.D.H. Bhadeshia, eds., The Institute of Materials London, 1998, p. 494-513.

Gedeon S.A., Eagar T.W., "Resistance spot welding of galvanized steel, part II: Mechanisms of spot weld nugget formation", *Met. Trans. B*, vol. 17B, 1986, p 887-901.

Greenwood J.A., "Temperatures in spot welding", *British Welding Journal*, June 1961, p. 316-322.

Greitmann M.J., Rother K., "Numerical simulation of the resistance spot welding process using Spotwelder", *Mathematic Modelling of Weld Phenomena IV*, H. Cerjak and H.K.D.H. Bhadeshia, eds., The Institute of Materials London, 1998, p. 531-544.

Hahn O., Kurzok J.R., Rohde A., Thesing T., "Computer-aided dimensioning of resistance-spot-welded and mechanically joined components", *Schweissen und Schneiden*, vol. 51, N°1, 1999, p 17-23 and E13-E16.

Huh H., Kang W.J., "Electrothermal analysis of electric resistance spot welding processes by a 3-D finite element method", *Journal of Materials Processing Technology*, Vol. 63, 1997, p. 672-677.

ISO, "Resistance welding – Weldability – Part 2: Alternative procedures for the assessment of sheet steels for spot welding", prEN ISO 18278-2, 2003.

Koppenhoefer K., Crompton J.S., Wung P., Failure of spot welded coupons, Edison Welding Institute, November 2000, summary report SR0017.

Le Meur G., Etude de la condition de liaison thermique à une interface de contact solide-solide siège d'une dissipation par effet Joule: Application au soudage par points, PhD. Thesis, Ecole Polytechnique de l'Université de Nantes, 2002.

Matsuyama K.I., Obert R., Chun J.H., "Inverse method for measuring weld temperatures during resistance spot welding", *International Institute of Welding*, Doc. N° III-1214-02, 2002.

Nied H.A., "The finite element modelling of the resistance spot welding process", *Welding Research Supplementary*, April 1984, p. 123s-132s.

Rice W., Funk E.J., "An analytical investigation of the temperature distributions during resistance welding", *Welding Journal*, 46(4), 1967, p. 175s-186s.

Robin V., Sanchez A., Dupuy T., Soigneux J., Bergheau J.M., "Numerical simulation of spot welding with special attention to contact conditions", *Mathematic Modelling of Weld Phenomena VI*, H. Cerjak and H.K.D.H. Bhadeshia, eds., The Institute of Materials London, 2002.

Silny J., Aspacher K.G., Dilthey U., Heidrich J., Ahrend M., "Elektromagnetische Umweltverträglichkeit von Widerstandspunktschweissanlagen", *Schweissen und Schneiden*, H. 5, 2001, p. 264-271.

Sudnik V.K., Erofeev, Kudinov R.A., Dilthey U., Bohlmann H.C., "Simulation of resistance spot welding using SPOTSIM software", *Welding International*, 13(2), 1999, p. 141-146.

Srikunwong C., Dupuy T., Bienvenu Y., "Numerical Simulation of Resistance Spot Welding Process using FEA Technique", *Proceedings of 13th International Conference on Computer Technology in Welding*, June 2003, Orlando, FL.

Srikunwong C., Dupuy T., Bienvenu Y., "Influence of Electrical-Thermal Physical Properties in Resistance Spot Welding Modelling", *7th International Seminar Numerical Analysis of Weldability*, H. Cerjak and H.K.D.H. Bhadeshia, eds., The Institute of Materials London, Oct. 2003, (Paper is submitted).

Tang H., Hou W., Hu S.J., Zhang, H. "Force characteristics of resistance spot welding of steel", *Welding Research Supplementary*, July 2000, p. 175s-183s.

Tang H., Hou W., Hu S.J., Zhang H., Feng Z., Kimchi M., "Influence of welding machine mechanical characteristics on the resistance spot welding process and weld quality", *Welding Research Supplementary*, May 2003, p. 116s-124s.

Thièblemont E., Modélisation du Soudage par Points, PhD. Thèse, L'Institut National Polytechnique de Lorraine, 1992.

Tsai C.L., Dai W.L., Dickinson D.W., Papritan J.C., "Analysis and development of a real-time control methodology in resistance spot welding", *Welding Journal*, dec. 1991, p. 339s-351s.

Vichniakov A., Herold H., « Simulation of the projection welding process », *Mathematical Modelling of Weld Phenomena 5*, H. Cerjak and H.K.D.H. Bhadeshia eds., The Institute of Metals, London, 2001, p 961-982.

Vogler M., Investigation of resistance spot welding formation, PhD. Thesis, Stanford University, Dec. 1992.

Vogler M. and Sheppard S., "Electrical contact resistance under high loads and elevated temperatures", *Welding Research Supplement*, June 1993, p. 231s-238s.

Watt D.F., Coon L., Bibby M., Goldak J., Henwood C., "An algorithm for modelling microstructural development in weld heat-affected zones (Part A) Reaction kinetics", *Acta metallurgica*, Vol. 36, No. 11, 1988, p. 3029-3035.

Zhang W., Bay N., "Finite element modelling aided process design in resistance welding", *Proceedings of 8th International Conference: Computer Technology in Welding*, University of Liverpool, June 1998.